APPROXIMATE SOLUTION OF THE BFKL EQUATION APPLICABLE AT HERA

P. Desgrolard (1), L. Jenkovszky (2), F. Paccanoni (3)

- (¹) Institut de Physique Nucléaire de Lyon, IN2P3-CNRS et Université Claude Bernard, F69622 Villeurbanne Cedex, France.
- (2) Bogolyubov Institute for Theoretical Physics, National Academy of Sciences of Ukraine, Kiev-143, Ukraine.
- (3) Dipartimento di Fisica, Universitá di Padova, Istituto Nazionale di Fisica Nucleare, Sezione di Padova, via F.Marzolo, I-35131 Padova, Italy.

Abstract

We suggest a formula interpolating between the known asymptotic regimes of the BFKL equation as the approximate solution of that equation. The parameters appearing in this interpolation are fitted to the data on deep inelastic scattering in a wide range of the kinematical variables. Care is taken of the large-x domain as well, outside the HERA kinematical region. The boundaries and the interface between various dynamical regimes are also studied.

 $^{^{1}\}mathrm{E\text{-}mail:}$ desgrolard@ipnl.in2p3.fr

²E-mail: jenk@bitp.kiev.ua

³E-mail: paccanoni@pd.infn.it

1 INTRODUCTION

The Balitski-Fadin-Kuraev-Lipatov (BFKL) equation [1] is a relativistic bound state equation for two reggeized gluons. Although first applications concerned $\gamma\gamma$ scattering, the equation originally was derived for the hadronic (on mass shell) scattering amplitude in quantum chromodynamics (QCD) at high energies \sqrt{s} and fixed momentum transfer $\sqrt{-t}$ in the leading logarithmic approximation (LLA), implying the collection of all terms of the type $(\alpha_s \ln s)^n$, α_s being the QCD ("running") coupling constant. In this approximation, the total cross section increases rapidly, as

$$\sigma_{tot}^{LLA} \sim \frac{s^{\omega}}{\sqrt{\ln s}},$$
 (1.1)

where ω is (in the LLA) the position of the rightmost singularity in the complex angular momentum plane of the t-channel partial wave with the vacuum quantum numbers (Pomeranchuk singularity), given by

$$\omega = \frac{g^2}{\pi^2} N \ell n 2 \tag{1.2}$$

for the gauge group SU(N) (N=3 in QCD), with a gauge coupling constant $g = \sqrt{4\pi\alpha_s}$.

Simply stated, the hope is that by solving the BFKL equation, one will be able to restrict the freedom available in the Regge pole theory, namely to determine the form of the leading singularities in the angular momentum plane, the form and the values of the parameters of the vacuum (Pomeranchuk) trajectory etc... Of all these ambitious expectations only (1.1) was of practical use, although still subject of uncertainties coming from the convergence condition $\alpha_s \ln s \leq 1$ and kinematical limitations. Any extrapolation of α_s to t=0 should have discouraged the direct application of (1.1) to fit measured hadronic cross sections. Really, even with a conservative value of $\omega \geq 1.3$, optimistic attempts in fitting data in the late 70-ies and early 80-ies were soon abandoned.

With the appearence of large virtualities, a new "hard" scale at HERA offered new possibilities for the interpretation of the "QCD-Pomeron": most of the HERA results were claimed to confirm the existence of a "hard" Pomeron, manifest in the rapid rise of the structure functions, photoproduction of heavy vector mesons etc... While the experimental results were claimed to confirm quantitatively the predictions of the BFKL equation (rapid rise in s or in s o

What remains now from the "QCD Pomeron" is that it has a complicated j-plane structure and the rightmost (leading) singularity is located somewhere above unity. Since there is little hope that the whole perturbative series will ever be summed, and waiting for possible numerical solutions of the BFKL equation, all we can do now is to start from a "supercritical" ($\alpha(0) > 1$) Pomeron and adjust it to the data.

An important point to be mentioned here is that the above Pomeron is meant at the Born level, *i.e.* it should be subject to a subsequent unitarization procedure. Such a procedure is very complicated already in case of hadronic (on mass shell) reactions and becomes even more tricky as $Q^2 \neq 0$. A practical way out from this situation may be along the lines suggested in [3], namely by introducing a Q^2 -dependent "effective" trajectory of a single, simple, factorizable supercritical Pomeron pole, absorbing the effect of its complicated j-plane structure as well as those from the possible unitarity effects (that cannot be calculated exactly anyway) in the form

of its "effective" trajectory. The free parameters are then adjusted to the experimental data. All what remains now from QCD is that $\alpha(0) > 1$, which reflects the present status of the solutions of the BFKL equation at finite Q^2 .

However, the solution of the BFKL equation is known exactly in the asymptotic, $Q^2 \to \infty$ limit as well, namely

$$F_2(x, Q^2) \sim \exp\sqrt{\gamma_1 \ell n(1/x) \ell n \ell n Q^2}.$$
(1.3)

We suggest to use the two known solutions of the BFKL equation, (1.1) and (1.3) as boundary conditions and interpolate between these two by employing a minimal number of additional parameters. In our opinion this is the simplest solution of the problem, yet applicable to realistic processes at arbitrary values of Q^2 . By fitting the parameters to the experimental data, we hope to be consistent with unitarity and find the boundaries of different dynamical regimes, namely those governed by the BFKL equation or QCD evolution.

In our previous paper [4] we have already investigated such an interpolation within the GLAP evolution equation [5] by assuming the "BFKL Pomeron" (1.1) to be the input, subject of a subsequent evolution. Actually, the asymptotic solutions of both the BFKL and GLAP equations have the same form (1.3) but the relevant paths may be different. Aiming at a high quality and reliable fit at small x, we have substantially improved as compare to our previous paper [4] the quality and range of the fits in the ("subsidiary") large-x domain. Still, the real paths of the solutions remain ambiguous for two main reasons: uncertainties in the low Q^2 , nonperturbative behavior (remaining outside of both the GLAP and BFKL equations) and unitarization (to effect both solutions), whose role increases with increasing Q^2 and decreasing x. Further work in this direction is needed.

Our paper is organized as follows. In Sect. 2 we present our interpolating solution, in Sec. 3 we find the value of the adjustable parameters by fitting to the data on deep inelastic scattering; our conclusions are given in Sect. 4.

2 THE MODEL

We use the standard kinematic variables to describe deep inelastic scattering (DIS):

$$e(k) + p(P) \rightarrow e(k') + X$$
, (2.1)

where k, k', P are the four-momenta of the incident electron, scattered electron and incident proton. Q^2 is the negative squared four-momentum transfer carried by the virtual exchanged photon (virtuality)

$$Q^2 = -q^2 = -(k - k')^2. (2.2)$$

x is the Björken variable

$$x = \frac{Q^2}{2P \cdot q} \,. \tag{2.3}$$

W is the center of mass energy of the (γ^*, p) system, related to the above variables by

$$W^2 = Q^2 \frac{1-x}{x} + m_p^2 , (2.4)$$

with m_p being the proton mass.

2.1 Structure function for low x and all Q^2

According to [4], we adopt the following ansatz for the small-x singlet part (labelled by the upper index S, 0) of the proton structure function, interpolating between the "soft" (1.1) and "hard" (1.3) regimes

$$F_2^{(S,0)}(x,Q^2) = G(Q^2) e^{\Delta(x,Q^2)},$$
 (2.5)

with

$$G(Q^2) = A \left(\frac{Q^2}{Q^2 + a}\right)^{1 + \widetilde{\Delta}(Q^2)},$$
 (2.6)

$$\widetilde{\Delta}(Q^2) = \epsilon + \gamma_1 \ell n \left(1 + \gamma_2 \ell n \left[1 + \frac{Q^2}{Q_0^2} \right] \right), \tag{2.7}$$

and

$$\Delta(x,Q^2) = \left(\tilde{\Delta}(Q^2) \, \ln \frac{1}{x}\right)^{f(Q^2)},\tag{2.8}$$

$$f(Q^2) = \frac{1}{2} \left(1 + e^{-Q^2/Q_1^2} \right). \tag{2.9}$$

The function $f(Q^2)$ has been introduced in order to provide for the transition from the Regge behavior, where $f(Q^2) = 1$, to the asymptotic solution (1.3) of the BFKL evolution equation where $f(Q^2) = 1/2$. Alternative choices for this function, satisfying the boundary conditions, cannot be excluded, but we find our way of interpolation via (2.9) to be the simplest possible.

It is customary to define an "effective" Pomeron intercept $\alpha_{\mathcal{P}}^{eff}$, which is in gereral x- and Q^2- dependent, by rewriting the proton SF, introducing an "effective power" $\Delta^{eff}(x,Q^2)$

$$F_2^{(S,0)}(x,Q^2) = G_1(Q^2) \ x^{-\Delta^{eff}(x,Q^2)} \ , \tag{2.10}$$

where the two effective quantities satisfy

$$\Delta^{eff}(x, Q^2) = \alpha_{\mathcal{P}}^{eff}(x, Q^2) - 1 . {(2.11)}$$

This definition with our parametrization leads to the identification

$$G_1(Q^2) = G(Q^2), \qquad \Delta^{eff}(x, Q^2) = \frac{\Delta(x, Q^2)}{\ell n_T^{\frac{1}{2}}}.$$
 (2.12)

It is worth noting that, in the limit

$$f(Q^2) \simeq 1$$
, i.e. when $Q^2 \ll Q_1^2$, (2.13)

the proton singlet (Pomeron component) SF reduces to

$$F_2^{(S,0)}(x,Q^2 \ll Q_1^2) \simeq G(Q^2) x^{-\widetilde{\Delta}(Q^2)}$$
 (2.14)

We recover the standard (Pomeron-dominated) Regge behavior (with a Q^2 -dependence in the effective Pomeron intercept). Consequently, within this approximation

$$\Delta^{eff}(x, Q^2) \simeq \widetilde{\Delta}(Q^2) . \tag{2.15}$$

Therefore, at small and moderate values of Q^2 (to be specified from the fits (see below), the exponent $\tilde{\Delta}(Q^2)$ may be interpreted as a Q^2 -dependent (and of course x-independent) effective power.

By construction, the model (singlet component) has the following Q^2 limits : - a) $Q^2 \to \infty$, fixed x:

$$F_2^{(S,0)}(x,Q^2\to\infty)\to A \exp\left(\sqrt{\gamma_1\ell n\ell n\frac{Q^2}{Q_0^2}\ell n\frac{1}{x}}\right)$$
, (2.16)

which is the asymptotic solution of the BFKL and GLAP evolution equation (see Sect.1).

- b) $Q^2 \to 0$:

$$F_2^{(S,0)}(x,Q^2 \to 0) \to A \ e^{\Delta(x,Q^2 \to 0)} \ \left(\frac{Q^2}{a}\right)^{1+\Delta(Q^2 \to 0)}$$
 (2.17)

with

$$\widetilde{\Delta}(Q^2 \to 0) \to \epsilon + \gamma_1 \gamma_2 \left(\frac{Q^2}{Q_0^2}\right) \to \epsilon,$$
 (2.18)

$$f(Q^2 \to 0) \to 1,$$
 (2.19)

whence

$$F_2^{(S,0)}(x,Q^2 \to 0) \to A \left(\frac{1}{x}\right)^{\epsilon} \left(\frac{Q^2}{a}\right)^{1+\epsilon} \propto Q^2 \to 0 ,$$
 (2.20)

as required by gauge invariance.

Apart from the (singlet, or Pomeron) component, a non-singlet component (sub-leading, or secondary Reggeons in terms of the Regge pole model) is also present at small x. Their contribution will be lumped in an "effective Reggeon" term, labelled by (NS,0) with the ρ , ω , f and A_2 reggeons absorbed in an effective trajectory with an intercept α_r , namely:

$$F_2^{(NS,0)}(x,Q^2) = H(Q^2) x^{1-\alpha_r}, \quad H(Q^2) = B\left(\frac{Q^2}{Q^2+b}\right)^{\alpha_r}.$$
 (2.21)

The resulting low-x proton SF becomes

$$F_2^{(0)}(x,Q^2) = F_2^{(S,0)}(x,Q^2) + F_2^{(NS,0)}(x,Q^2)$$
 (2.22)

2.2 Extension to large x

Our aim is to fix the free parameters appearing in our approximate solution of the BFKL equation (2.22). To this end, we could, in principle, fit (2.22) to the small-x data, where other contributions are negligeable. Whatever attractive, such a straighforward approach is not feasible since the small x domain where contributions to the SF other than (2.5) may be neglected is very narrow, making any fit unreliable. Moreover, the relevant limits depend on the models used, as shown explicitly in [6]. Therefore we extend our model (2.22) by a "large-x" part in order to have reasonable fits in a wide range of x.

In our previous paper [4] the relatively simple and efficient model of Capella *et al.* [3] (CKMT) was used for that purpose. Below, aiming a better fit to the large-x data, we extend that model, by introducing additional adjustable parameters as follows [7]

$$F_2(x,Q^2) = F_2^{(S,0)}(x,Q^2) \cdot (1-x)^{P(Q^2)} + F_2^{(NS,0)}(x,Q^2) \cdot (1-x)^{R(Q^2)}. \tag{2.23}$$

Similar to [7], we use the following Q^2 -dependent exponents of the large x factors (with 6 additional parameters)

$$P(Q^2) = p_{\infty} + \frac{p_0 - p_{\infty}}{1 + Q^2/Q_p^2}, \quad R(Q^2) = r_{\infty} + \frac{r_0 - r_{\infty}}{1 + Q^2/Q_r^2}.$$
 (2.24)

2.3 Total cross-section for (γ^*, p) scattering

The structure function is related to the total cross-section of virtual Compton scattering (or approximatively to the transverse cross-section, if the longitudinal component is neglected) by

$$\sigma_{tot}^{\gamma^*,p}(x,Q^2) = \frac{4\pi^2\alpha}{Q^2} \frac{1}{1-x} \left(1 + \frac{4m_p^2 x^2}{Q^2} \right) F_2(x,Q^2) = \sigma_{tot}^{\gamma^*,p}(W,Q^2), \tag{2.25}$$

where x is replaced by using (2.4).

In the limit $Q^2 \to 0$, the SF vanishes as Q^2 and we write the total cross-section for (γ, p) scattering (with real photons), as a function of the center of mass energy W

$$\sigma_{tot}^{\gamma,p}(W) = 4\pi^2 \alpha \lim_{Q^2 \to 0} \left[\frac{F_2(x = Q^2/W'^2, Q^2)}{Q^2} \right]$$

$$= 4\pi^2 \alpha \left(A \ a^{-1-\epsilon} \ W'^{2\epsilon} + B \ b^{-\alpha_r} \ W'^{2(\alpha_r - 1)} \right) , \qquad (2.26)$$

with $W'^2 = W^2 - m_p^2$.

3 FITTING TO THE DATA; RESULTS

In our fitting procedure the experimental data sets from "H1" [8, 9, 10], "ZEUS" [11, 12, 13], "E665" [14], "NMC" [15], SLAC[16], "BCDMS" [17] for the proton structure function $F_2(x, Q^2)$ were used as well as data points [18] on the (γ, p) total cross-section $\sigma_{tot}^{(\gamma,p)}(W)$, in the kinematical region with $0 \le Q^2 \le 5000~{\rm GeV^2}, \ 0 < x \le 0.75, \ W \ge 3~{\rm GeV}$. The total number of data for this "complete" ensemble is 1253 (see Table 1).

The resulting fits may be commented as follows.

The use in [4] of an "economic" (only 8 free parameters) large-x extension a la CKMT[3] resulted in good fits ($\chi^2_{d.o.f} \sim 0.67$) within a rather limited domain in $x \leq 0.1$, with a selection of about 310 data points (mainly those of the low x H1 data).

Better fits at large x (including the BCDMS and SLAC data) can be achieved (at the price of 6 additional parameters with the large x extension, presented above. Namely, we obtained $\chi^2_{d.o.f} \sim 1.16$, distributed among each subset of data as shown in Table 1. This is a considerable improvement with respect to the small x, all Q^2 results of [4]. Interestingly, the present improvement of the large-x behavior has little effect on the values of the parameters governing the low x behavior and fitted previously [4]. As noted, 6 new parameters were introduced in our present version of the model (see Table 2). Among a total of 16 parameters, 14 are free (instead of 8 in [4]), the remaining 2 being fixed in the following way:

- 1. Similar to [4], we choose the "canonical" value [19] $\epsilon = 0.08$;
- 2. Similar to [4], we estimate from QCD the parameter $\gamma_1 = 16N_c/(11 2f/3)$ with four flavours (f = 4) and three colors $(N_c = 3)$, it equals 5.76. It corresponds to the asymptotic regime (when $Q^2 \to \infty$, or $f(Q^2) \to 1/2$)), far away from the region of the fits, where f = 1, hence the value $\gamma_1 = \sqrt{5.76} = 2.4$ is more appropriate in the domain under consideration. Fits with γ_1 free confirm this choice.

To compare with, the proton structure function and (γ^*, p) cross section are calculated in the ALLM model [20] in the whole experimentally investigated kinematical range. The ALLM fits to the data are good $(\chi^2_{d.o.f} \sim 1.1$, recalculated) with a total of 23 adjustable parameters. This is also to be compared with the 21 parameters used in [7], where a quite good fit (with only a slightly better $\chi^2_{d.o.f}$) is also presented.

The results of our fits for the structure function versus x for fixed selected Q^2 are shown in Figs. 1-2.

The total cross section for real photons on protons as function of W^2 is displayed in Fig. 3. The agreement with the data is impressive except may be for the SF reported at the highest Q^2 -value (=5000 GeV²). We recall once again that this result is obtained with 14 free parameters.

Q-slope as a function of x

Known as a useful tool in the sudies of low x region, the derivative of the SF with respect to ℓnQ^2

$$B_Q(x, Q^2) = \frac{\partial F_2(x, Q^2)}{\partial (\ell n Q^2)}$$
(3.1)

(Q-slope for brevity) measures the amount of the scaling violation and eventually shows the transition from soft to hard dynamics. It was recently extracted from the HERA data [13], where the variables x and Q^2 are strongly correlated, because it is implied that, for a limited acceptance (as it is the case in the HERA experiments) and for a fixed energy, one always has a limited band in Q^2 at any given x, with average $< Q^2 >$ becoming smaller for smaller x.

From the theoretical point of view however, this derivative depends on two variables $(x \text{ and } Q^2)$ which are quite independent and one is not restricted to follow a particular path on the surface representing the Q-slope. That is why we discussed in [4] the Q-slope as a three-dimensional quantity. Here we adopt a more pragmatic attitude and we only compare in Fig. 4 the predictions of our model with the available experimental results for the special experimental set of (x,Q^2) chosen in [13]. Our predictions are quite in agreement with the data, as it may be expected from a good fit of the structure function implying also agreement with its experimental derivatives: an increasing Q-slope when x decreases down to $\sim 10^{-4}$, then a "turn over": the slope decreasing at lower x (or Q^2) values. Notice that the turn over point, located at $Q^2 \sim 2 \text{ GeV}^2$, may be related to the different behaviors of the gluon and $q\bar{q}$ sea distributions.

x-slope as a function of Q^2

The derivative of the logarithm of the SF with respect to $\ell n1/x$

$$B_x(x,Q^2) = \frac{\partial \ell n F_2(x,Q^2)}{\partial (\ell n(1/x))}$$
(3.2)

(x-slope for brevity), when measured in the Regge region, can be related (for low x) to the Pomeron intercept. In Fig. 5, we compare the calculated x-slope with the quantity called "effective power" (λ_{eff}). In fact, the measured (x-dependent) quantity should not be confused with the "effective power" introduced in (2.10-12) ($\Delta^{eff}(x,Q^2)$ in our notation), it is really the x-slope. The agreement between experiment and theory is very good.

Finally, in Fig. 6 the Q^2 -dependence of this calculated derivative together with the power $\tilde{\Delta}$ (2.8) is shown for some low x - values. On the same figure, the behavior of the function

 $f(Q^2)$ (2.9) is also shown. In our model, Regge pole behavior is equivalent to the condition that $f(Q^2)$ is close to unity

$$f(Q^2) \approx 1 \; ; \quad \frac{\partial \ell n F_2}{\partial (\ell n (1/x))} \approx \Delta^{eff} \approx \tilde{\Delta} \; .$$
 (3.3)

This lower limit, marked on Fig. 6 (tentatively approximated within a 2 % accuracy for the function $f(Q^2)$), is located near 60 GeV². Until this landmark, the power $\tilde{\Delta}$ indeed remains very close to the x-slope. Beyond, Regge pole behavior is not valid (since $f \neq 1$) and $\tilde{\Delta}$ cannot be considered as the x-slope any more. On the other hand, the x-slope turns down as Q^2 increases, approaching its "initial value" of ≈ 0.1 at largest Q^2 and coming closer to the unitarity bound. Notably, at large Q^2 the derivative gets smaller as x decreases, contrary to the general belief that dynamics becomes harder for smaller x, but in accord with an observation made in [21]. Care should be however taken in interpreting the "hardness" of the effective power outside the Regge region.

The transition region occurs when $f(Q^2)$ goes from 1 to 1/2 *i.e.* in a band in Q^2 estimated between $\sim 60~{\rm GeV^2}$ and $\sim 5000~{\rm GeV^2}$.

4 CONCLUSIONS

The consequences of the present studies are manifold.

On the one hand, the present approximate solution of the BFKL equation ((1.5-9) with the parameters listed in Table 2) can be used in the future to compare it with the numerical solutions of this equation as soon as they will be available (and there is a strong need for such numerical solutions!).

Further, our interpolating formula may clarify the still open question: what is the Pomeron? While the answer is known within the context of the analytic S-matrix theory (that gave rise to the notion of the "Pomeron"), namely that it is an isolated moving j-plane singularity with vacuum quantum numbers and with $\alpha(0) = 1$, an alternative definition may arise from QCD, namely that the Pomeron is the solution of the BFKL equation. In that case the deviation from the simple $s^{\alpha(t,Q^2)}$ behavior may be indicative of the difference between the two. The model presented in this paper shows it.

Another aspect of the Pomeron studies is its "hardness" at low (or vanishing) Q^2 . It is well known (see e.g. [22]) that in the present energy range, the cross sections (or structure functions) can well be described by logarithmic functions as well (rather than powers in s (or 1/x)). Apart from numerical fits, this phenomenon has also a physical interpretation [23]: in the presently available energy range there is sufficient phase space available only for a finite (small) number of gluons rungs in the Pomeron ladder, each contributing with a power in ℓns (or $\ell n(1/x)$), resulting thus in a ℓns , ℓns , ... behavior of the cross sections (same for the SF). As repeatedly stressed, such logarithmic parametrizations, being equally efficient phenomenologically, have the advantage of being consistent with the unitarity bounds. Note that the extrapolation between the low Q^2 logarithmic behavior and high Q^2 asymptotics may be more complicated than that presented above. For that purpose the model of [24], combining the logarithmic behavior at $Q^2 = 0$ with a "supercritical" power behavior far off shall may be appropriate.

Finally, we remind that the "BFKL-Pomeron" presented in the present paper is not a direct solution of the BFKL equation. Instead, it interpolates betwen the two known asymptotic solutions of that equation and as such is a small step forwards with respect to those previously known. Our poor knowledge of other solutions (in different kinematical regions?) of the BFKL

equation shows on one hand the complexity of the problem, but on the other hand it is clear that further progress in theory cannot be achieved without a better understanding of such basic objects in high energy physics as the bound state of two gluons or the elastic scattering amplitude.

Acknowlegdments. We thank V. Fadin, E. Kuraev and L. Lipatov for numerous discussions on the Pomeron.

References

- [1] V. S. Fadin, E. A. Kuraev and L. N. Lipatov, Phys. Lett. B **60** 50 (1975);
 - E. A. Kuraev, L. N. Lipatov, V. S. Fadin, Sov. Phys. JETP 45, 199 (1977);
 - Y. Y. Balitzkij, L. N. Lipatov, Sov. J. Nucl. Phys. 28, 822 (1978);
 - L. N. Lipatov, Sov. Phys. JETP **63**, 904 (1986).
- [2] V. S. Fadin, L. N. Lipatov, BFKL Pomeron in the next-to-leading approximation, DESY-98-033, hep-ph/9802290 (1998); V. F. Fadin, Next-to-Leading Approximatin to the BFKL Pomeron, in Proc. of the "Hadrons-98", held in Crimea, ed. by L.Jenkovszky, 1998, p.167; G. Camici, M. Ciafaloni, hep-ph/9803389.
- [3] A. Capella, A. Kaidalov, C. Merino, J. Tran Thanh Van, Phys. Lett. B 337, 358 (1994). 0
- [4] P. Desgrolard, L. Jenkovszky, F. Paccanoni, Can the Pomeron (diffraction) be "soft" or "hard"?, in Proceedings of the international conference on strong interactions at high energies, Crimea (June 1998), edited by L. Jenkovszky (Kiev, 1998) p.78;
 - P. Desgrolard, L. Jenkovszky, F. Paccanoni, Eur. Phys. Jour. C (in press).
- [5] V. N. Gribov, L. N. Lipatov, Sov. J. Nucl. Phys. **15**, 438 and 675 (1972);
 - L. N. Lipatov, Sov. J. Nucl. Phys. **20** 94 (1975);
 - G. Altarelli, G. Parisi, Nucl. Phys. B **126**, 298 (1977).
- [6] M. Bertini, P. Desgrolard, Yu. M. Ilyn, Int. Journ. Phys. 1, 45 (1995).
- [7] P. Desgrolard, S. Lengyel, E. Martynov, Eur. Phys. Jour. C (in press).
- [8] T. Ahmed *et al.* H1 collaboration, Nucl. Phys. B **439**, 471 (1995).
- [9] S. Aid et al. H1 collaboration, Nucl. Phys. B 470, 3 (1996).
- [10] C. Adloff *et al.* H1 collaboration, Nucl. Phys. B **497**, 3 (1997).
- [11] M. Derrick et al. ZEUS collaboration, Zeit. Phys. C 72, 399 (1996).
- [12] J. Breitweg *et al.* ZEUS collaboration, Phys. Lett. B **407**, 432 (1997).
- [13] J. Breitweg et al. ZEUS collaboration, ZEUS results on the measurement and phenomenology of F_2 at low x and low Q^2 , DESY-98-121, hep-ex/9809005.
- [14] M.R. Adams et al. E665 collaboration, Phys. Rev. D 54, 3006 (1996).

- [15] M. Arneodo et al. NMC collaboration, Nucl. Phys. B 483, 3 (1995).
- [16] SLAC-PUB 317 (1990);L. W. Whitlow et al., Phys. Lett. B 282, 475 (1992).
- [17] A. C. Benvenuti et al. BCDMS collaboration, Phys. Lett. B 223, 485 (1989).
- [18] D. O. Caldwell et al., Phys. Rev. D 7, 1384 (1975) and Phys. Rev. Lett. 40, 1222 (1978);
 M. Derrick et al. ZEUS collaboration, Zeit. Phys. C 63, 391 (1994);
 S. Aid et al. H1 collaboration, Zeit. Phys. C 69, 27 (1995).
- [19] H. Cheng, J. K. Walker, T. T. Wu, Phys. Lett. B 44, 97 (1973);
 A. Donnachie, P. V. Landshoff, Phys. Lett. B 296, 493 (1975).
- [20] H. Abramowicz, E. Levin, A. Levy, U. Maor, Phys. Lett. B 269, 465 (1991);
 H. Abramowicz, A. Levy, DESY 97-251 and hep-ph/9712415, (1997).
- [21] A. De Roeck, E. A. De Wolf, Phys. Lett. B 388, 188 (1996).
- [22] L. Jenkovszky, F. Paccanoni, E. Predazzi, in Proceedings of the "Blois" Conference, Elba, 1991, Nucl Phys. B (Proc. Supplement) 25, 80 (1992).
 - P. Desgrolard, M. Giffon, L. Jenkovszky, A. Lengyel, E. Predazzi, Phys. Lett. B **309**, 191 (1993);
 - M. Bertini, P. Desgrolard, M. Giffon, L. Jenkovszky, F. Paccanoni, in Strong Interaction at Long Distances, edited by L. L. Jenkovszky (Hadronic Press, Palm Harbor, 1995) p.181;
 - L. L. Jenkovszky, E. S. Martynov, F. Paccanoni, Regge behavior of the nucleon structure functions, PFPD 95/TH/21, 1995;
 - L. L. Jenkovszky, A. Lengyel, F. Paccanoni, Nuovo Cim. (in press).
- [23] L. Jenkovszky, A. Kotikov, F. Paccanoni, Z. Phys. C Particles and Fields 63, 131 (1994).
- [24] M. Bertini, M. Giffon, E. Predazzi, Phys. Lett. B 349, 561 (1995).

Observable	Number of points	χ^2	χ^2
Experiment – year of pub., Ref			[4]
F_2^p			
H1 - 95 [8]	93 (0 in [4])	77	_
H1 - 96 [9]	193	149	110
H1 - 97 [10]	44	55	20
ZEUS - 96 [11]	188 (0 in [4])	256	_
ZEUS - 97 [12]	34 (0 in [4])	13	_
ZEUS - 98 [13]	44 (0 in [4])	28	_
E665 - 96 [14]	91 (0 in [4])	101	_
NMC - 95 [15]	156 (0 in [4])	177	_
SLAC - 90/92 [16]	136 (0 in [4])	145	_
BCDMS - 89 [17]	175 (0 in [4])	257	_
$\sigma_{tot}^{\gamma,p}$ [18]	99 (73 in [4])	177	73
Total	1253 (310 in [4])	1434	203
$\chi^2 / d.o.f.$	_	1.16	0.67

Table 1.

Observables used in the fitting procedure. The complete available experimental kinematical range is taken into account for Q^2 (i.e. $0. \le Q^2$ (GeV²) ≤ 5000 , x (2. $10^{-6} \le x \le 0.75$), with the lower limit $W \ge 3$ GeV.

Also shown is the distribution of the partial χ^2 for each subset of data used in our fit with the parameters listed in Table 2. The results from [4] are also shown.

low x		
A = .1365		
$a (GeV)^2 = .2372$		
$\gamma_2 = .02158$		
$Q_0^2 (GeV)^2 = .1991$		
$\mathbf{Q_1^2} \; (\text{GeV})^2 = 1490.$		
B = 1.944		
$\mathbf{b} \; (\text{GeV})^2 = 1.804$		
$\alpha_{\mathbf{r}} = .3603$		
$\mathbf{large} \ x$		
$Q_p^2 (GeV)^2 = .1864$		
$\mathbf{p_0} = -26.32$		
$\mathbf{p}_{\infty} = 10.52$		
$Q_r^2 (GeV)^2 = 13.86$		
$r_0 = 2.601$		
$\mathbf{r}_{\infty} = 3.846$		

Table 2.

Free parameters used in our fit. The non-fitted values are $\epsilon = 0.08$ (fixed from [19]) and $\gamma_1 = 2.4$ (suggested by QCD).

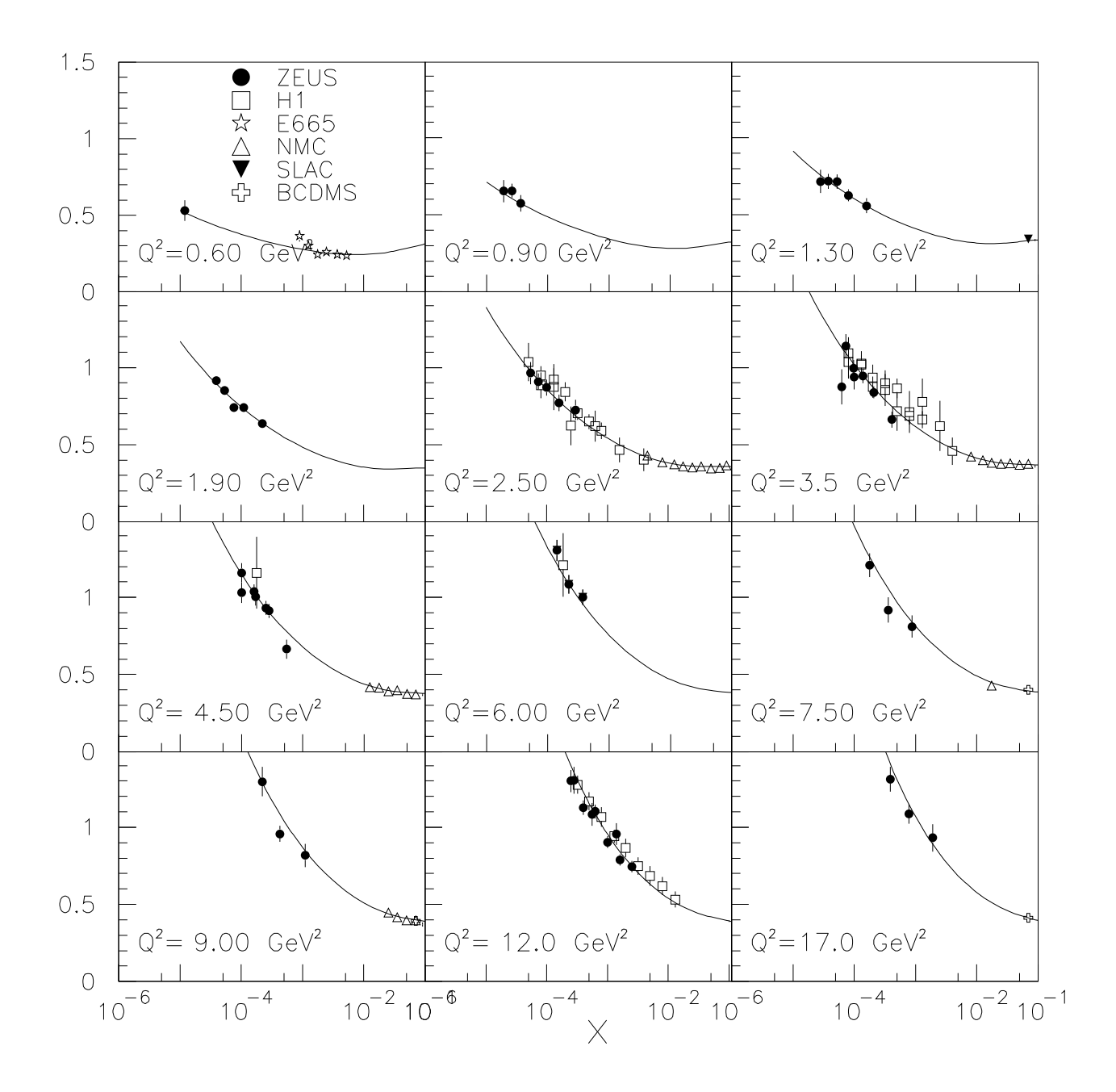


Fig. 1 Proton structure function $F_2(x, Q^2)$ as a function of x at low Q^2 . The data shown are listed in Table 1, the error bars represent the statistical and systematic errors added in quadrature, the solid curves are the results of our fit (the parameters are listed in Table 2).

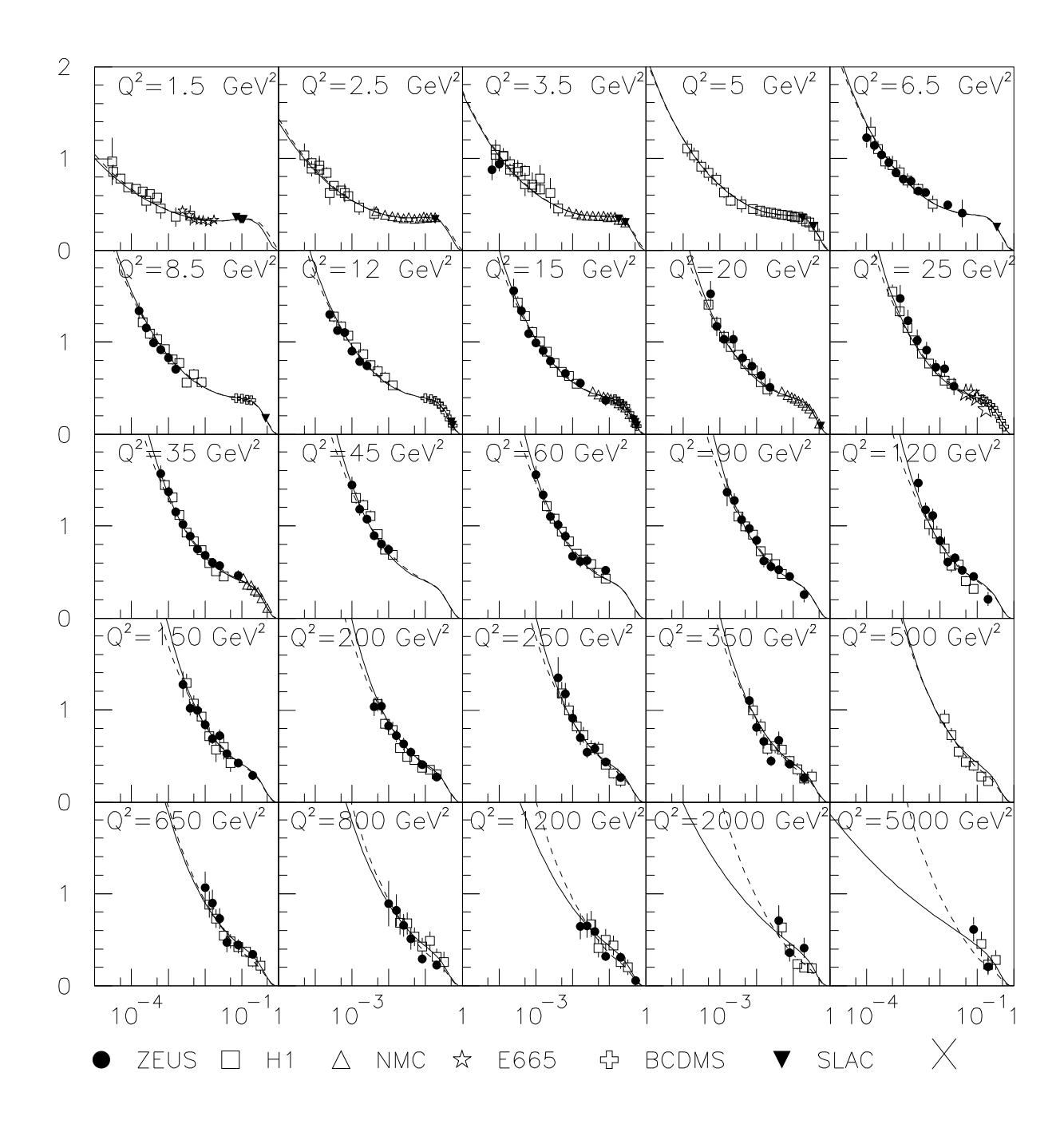


Fig. 2 Proton structure function $F_2(x, Q^2)$ as a function of x at various values of Q^2 (see also Fig. 1). The dashed lines are the results of the ALLM model [20].

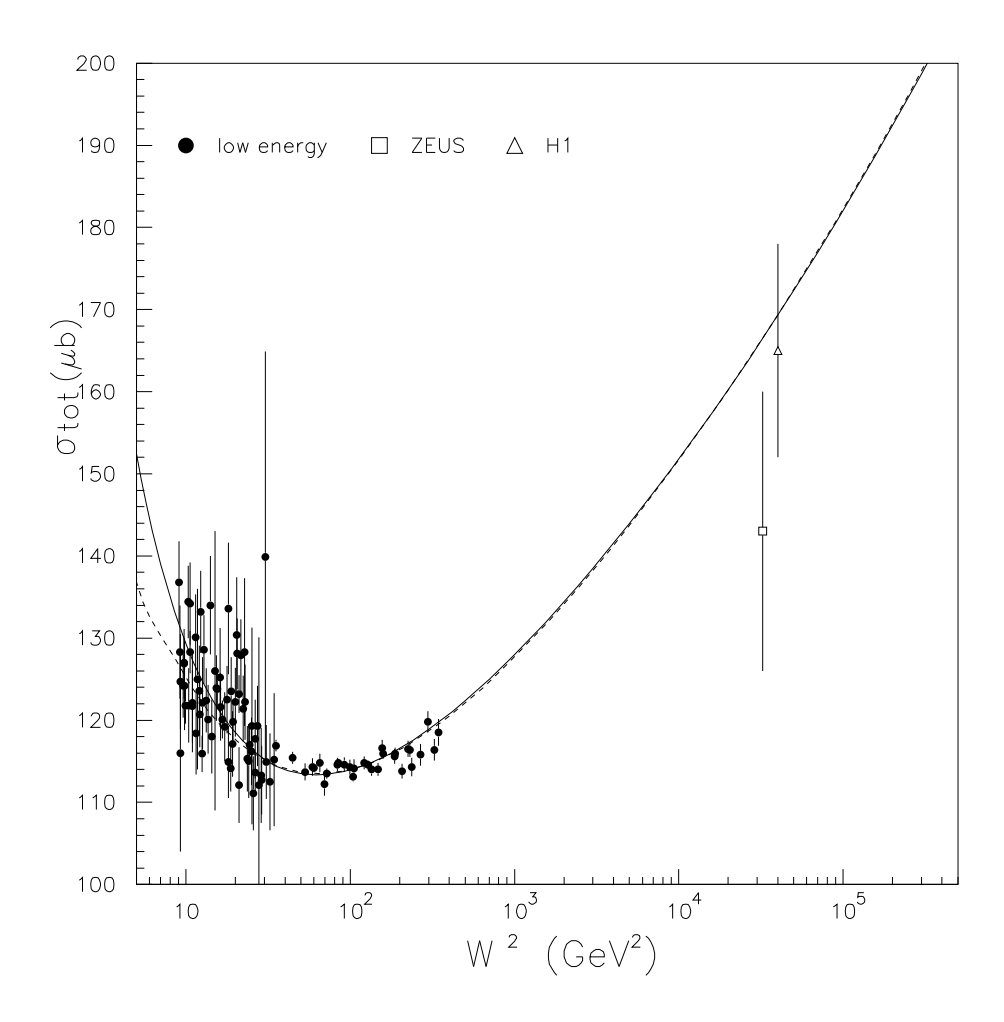


Fig. 3. Limiting case to the real photon-proton total cross-section $\sigma_{tot}^{(\gamma,p)}$ as a function of W^2 , square center of mass energy (see also Fig. 1). The dashed lines are calculations from the ALLM model [20].

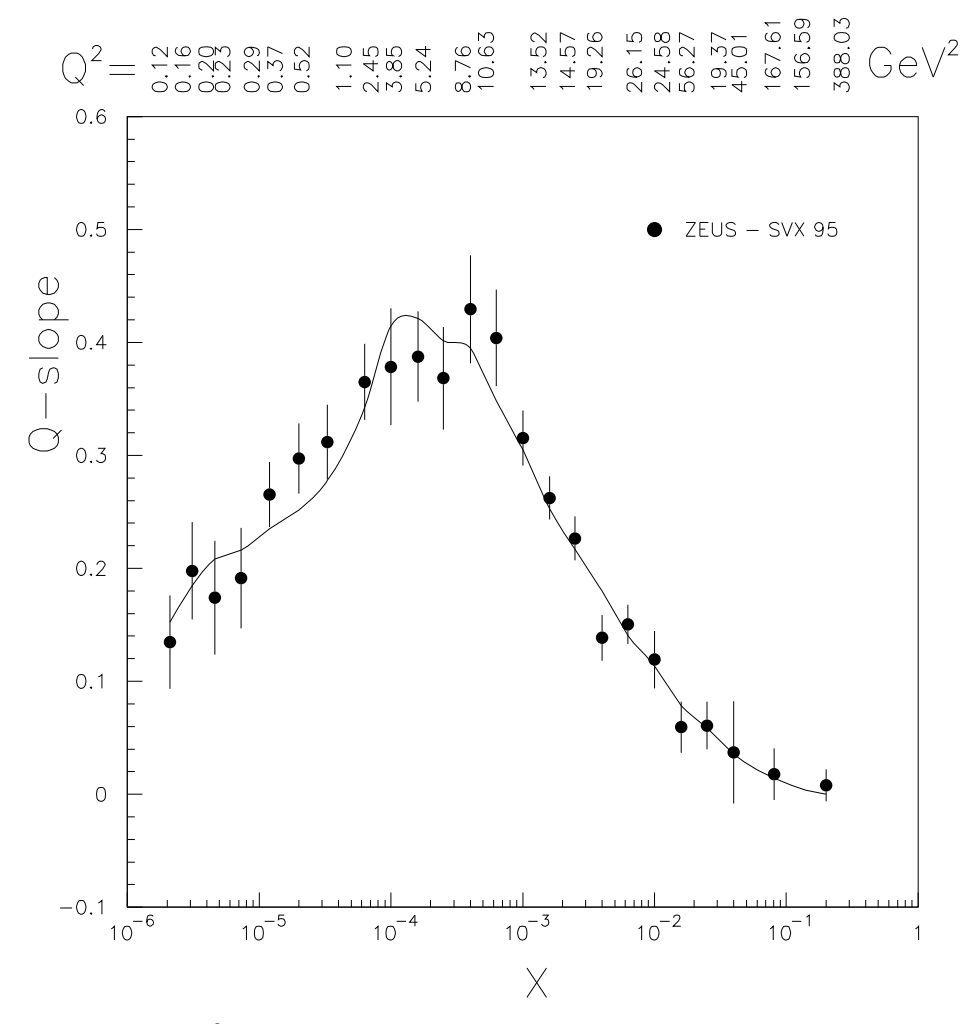


Fig. 4. Q-slope $=\frac{\partial F_2(x,Q^2)}{\partial \ell n Q^2}$ as a function of x (for the indicated Q^2 values). The experimental points are from [13]. The predictions in the present model are given in continuous line.

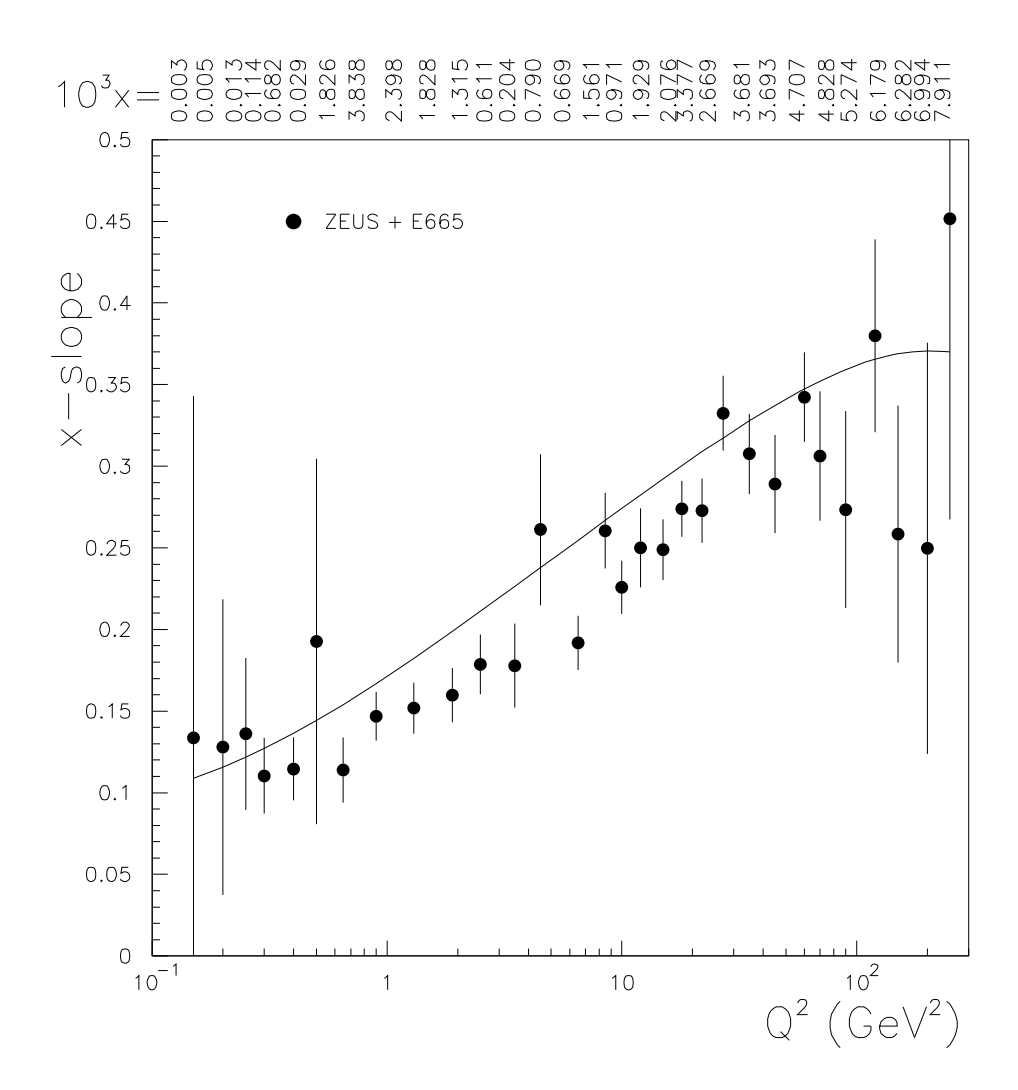


Fig. 5. $\lambda_{eff}(< x >, Q^2)$ experimental points from [13] as a function of Q^2 (for the indicated < x > values), compared with the calculated x- slope values $= \frac{\partial \ell n F_2(x,Q^2)}{\partial (\ell n(1/x))}$. The predictions in the present model are given in the approximation including only the low x Pomeron contribution (2.5).

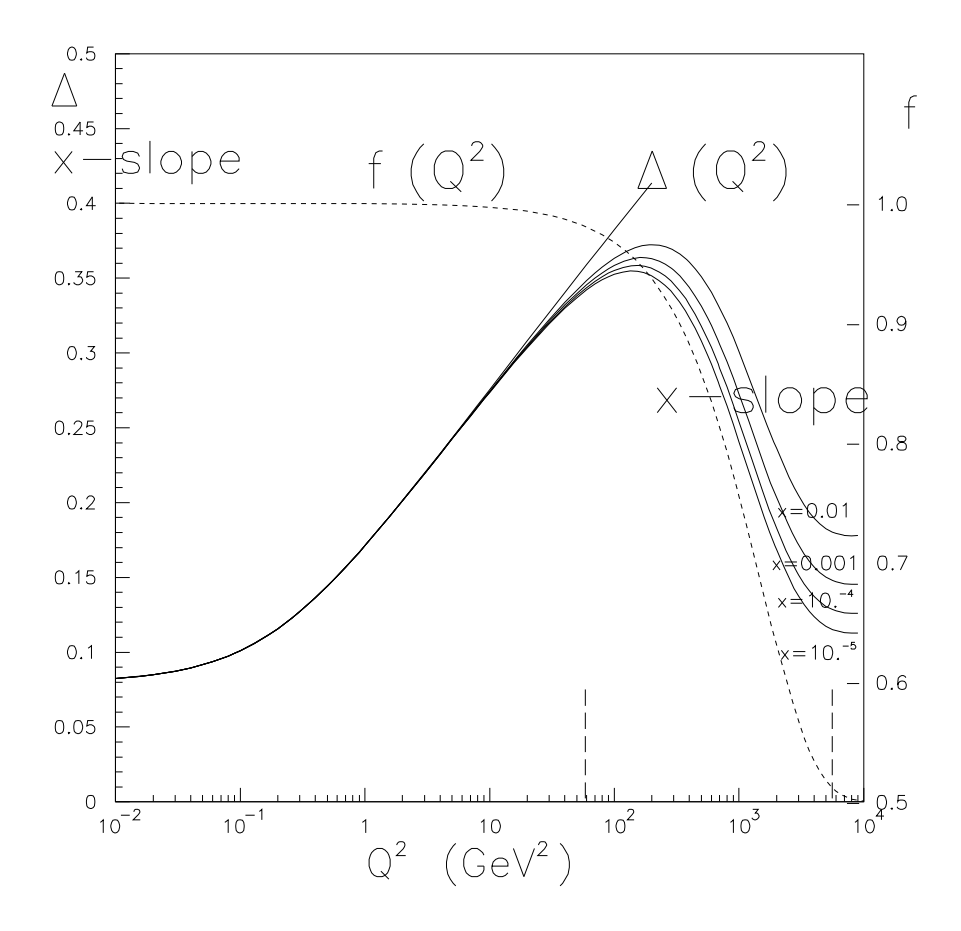


Fig. 6. x-slope = $\frac{\partial \ell n F_2(x,Q^2)}{\partial (\ell n(1/x))}$ as a function of Q^2 (for the indicated x values). The predictions in the present model (solid line) are calculated in the low x Pomeron approximation (see Fig. 5). On the same left scale the exponent $\tilde{\Delta}$ (2.8), equivalent to the Pomeron intercept-1 when $f(Q^2) \approx 1$ is also plotted. This function $f(Q^2)$ is also shown in dash line (right scale). The estimated transition region is between the vertical landmarks (see the text).